

Functional and Structural Basis of Carnitine Palmitoyltransferase 1A Deficiency*

Received for publication, September 11, 2003, and in revised form, September 26, 2003
Published, JBC Papers in Press, September 29, 2003, DOI 10.1074/jbc.M310130200

Stéphanie Gobin^{‡§¶}, Laure Thuillier^{‡§}, Gerwald Jogl^{||}, Audrey Faye[‡], Liang Tong^{||}, Mihaiti Chi[§], Jean-Paul Bonnefont[§], Jean Girard[‡], and Carina Prip-Buus^{‡**}

From the [‡]Département d'Endocrinologie, Institut Cochin, INSERM U567, CNRS Unité Mixte de Recherche 8104, Université René Descartes, 24 Rue du Faubourg Saint-Jacques, 75014 Paris, France, [§]INSERM U393, Hôpital Necker-Enfants malades, 149 Rue de Sévres, 75743 Paris Cedex 15, France, and the ^{||}Department of Biological Sciences, Columbia University, New York, New York 10027

Carnitine palmitoyltransferase 1A (CPT1A) is the key regulatory enzyme of hepatic long-chain fatty acid β -oxidation. Human CPT1A deficiency is characterized by recurrent attacks of hypoketotic hypoglycemia. We presently analyzed at both the functional and structural levels five missense mutations identified in three CPT1A-deficient patients, namely A275T, A414V, Y498C, G709E, and G710E. Heterologous expression in *Saccharomyces cerevisiae* permitted to validate them as disease-causing mutations. To gain further insights into their deleterious effects, we localized these mutated residues into a three-dimensional structure model of the human CPT1A created from the crystal structure of the mouse carnitine acetyltransferase. This study demonstrated for the first time that disease-causing CPT1A mutations can be divided into two categories depending on whether they affect directly (functional determinant) or indirectly the active site of the enzyme (structural determinant). Mutations A275T, A414V, and Y498C, which exhibit decreased catalytic efficiency, clearly belong to the second class. They are located more than 20 Å away from the active site and mostly affect the stability of the protein itself and/or of the enzyme-substrate complex. By contrast, mutations G709E and G710E, which abolish CPT1A activity, belong to the first category. They affect Gly residues that are essential not only for the structure of the hydrophobic core in the catalytic site, but also for the chain-length specificity of CPT isoforms. This study provides novel insights into the functionality of CPT1A that may contribute to the design of drugs for the treatment of lipid disorders.

Mitochondrial β -oxidation of long-chain fatty acids is a major source of energy production, especially during fasting, illness, or sustained exercise. Contrary to medium- and short-chain fatty acids that can cross the mitochondrial membranes by simple diffusion, long-chain fatty acids are imported into the mitochondrial matrix by the carnitine palmitoyltransferase (CPT,¹ EC 2.3.1.21) system (1, 2). The first component of this

system is CPT1, an integral mitochondrial outer membrane protein, which catalyzes the transfer of long-chain acyl group of the acyl-CoA ester to carnitine. CPT1 is tightly regulated by its physiological inhibitor malonyl-CoA, the first intermediate in fatty acid biosynthesis. This provides a mechanism for physiological regulation of β -oxidation in all mammalian tissues and for cellular fuel sensing based on the availability of fatty acids and glucose (1, 3, 4). By its strategic metabolic position, CPT1 represents a potential drug target for the treatment of metabolic disorders such as diabetes, insulin resistance, and coronary heart disease (5–7). However, the rational design of pharmacological molecules for altering CPT1 activity requires a better understanding of its structure-function relationships.

Three CPT1 isoforms with various tissue distribution and encoded by distinct genes have been identified (1, 2): a liver (CPT1A or L-CPT1) (8), a muscle (CPT1B or M-CPT1) (9), and a brain isoform (CPT1C) (10). During the past years, CPT1A has been the most investigated member of the acyltransferase family. CPT1A is anchored in the mitochondrial outer membrane by two transmembrane segments (TM1 and -2), its N terminus (residues 1–47) and C-terminal catalytic domain (residues 123–773) being located on the cytosolic face of mitochondria (11). The N-terminal domain (1–147 residues) was shown to be essential for mitochondrial import and for maintenance of a folded active and malonyl-CoA-sensitive conformation (12–14). Functional analysis of natural and/or engineered mutations in CPT1A strongly contributed to understanding the catalytic and regulatory mechanisms implied in the acyltransferase family (15–20). The recent three-dimensional structural models of the mouse and human carnitine acetyltransferase (CAT) provided critical insights into the molecular basis for fatty acyl chain transfer (21, 22). As CAT shares about 30–35% amino acid sequence identity to the other acyltransferases, its three-dimensional structure constitutes a more valuable tool than the model reported by Morillas *et al.* (16) to understand the molecular mechanisms responsible for the deleterious effects of natural mutations in human CPT1A.

CPT1A deficiency is a rare autosomal recessive disorder, characterized by severe episodes of hypoketotic hypoglycemia usually occurring after fasting or illness and beginning in early childhood (23). To date, eleven missense mutations of the 17 mutations identified in more than 20 reported CPT1A-deficient patients were analyzed by exogenous expression (24–28). Unfortunately, these mutations were not located within a structural model, impoverishing the informations they could bring regarding the structure-function relationships of this enzyme. In the present study, we investigated the molecular mechanisms responsible for the deleterious effects of five natural missense mutations identified in three CPT1A-deficient pa-

* This work was supported by grants from the Association Française contre les Myopathies. The costs of publication of this article were defrayed in part by the payment of page charges. This article must therefore be hereby marked "advertisement" in accordance with 18 U.S.C. Section 1734 solely to indicate this fact.

[¶] Recipient of a fellowship from the Fondation pour la Recherche Médicale.

** To whom correspondence should be addressed. Tel.: 33-1-53-73-27-04; Fax: 33-1-53-73-27-03; E-mail: prip-buus@cochin.inserm.fr.

¹ The abbreviations used are: CPT, carnitine palmitoyltransferase; CPT1A, liver isoform of human CPT1; CAT, carnitine acetyltransferase; TM, transmembrane; mt, mutant.

tients using both heterologous expression in *Saccharomyces cerevisiae* and a three-dimensional structure model of the human CPT1A that was created from our crystal structure of the mouse CAT (21).

EXPERIMENTAL PROCEDURES

Molecular Analysis of CPT1A-deficient Patients—Informed consent was obtained from all subjects. Case report of patient 2 (29) as well as molecular analysis of patients 1 and 3 (26, 27) have previously been reported. Fibroblasts from controls and patients were cultured as previously described (30) and were used to extract DNA according to standard methods and RNA using RNeasy Midi kit (Qiagen). Mutation analysis of patient 2 was performed at both cDNA and gDNA levels by sequencing approach, as previously described (26, 27).

Construction of Human CPT1A Mutants—pYeCPT1A-A275T, -A414V, -Y498C, and -G709E were constructed with the QuikChange site-directed mutagenesis kit (Stratagene) using pYeCPT1A-WT (26) as template that corresponds to the yeast expression vector pYeDP1/8–10 containing the full-length human CPT1A cDNA under control of the inducible GAL10 promoter. pYeCPT1A-A275T-A414V was constructed with a second step of mutagenesis creating the A414V mutation in pYeCPT1A-A275T. Mutations A275T, A414V, Y498C, and G709E were synthesized with pairs of mutagenized primers (sequences available upon request). cDNA of mutants were sequenced to assess the presence of the designed mutation as well as the absence of unwanted mutations. Plasmids were used to transform *S. cerevisiae* (haploid strain W303: MAT α , his3, leu2, trp1, ura3, ade2–1, and can1–100) (31).

Yeast Culture, Subcellular Fractionation, and Isolation of Yeast Mitochondria—Methods for yeast culture, subcellular fractionation, and isolation of yeast mitochondria were performed as previously described (31). Protein concentration was determined by the method of Lowry *et al.* (32) with bovine serum albumin as standard.

CPT Assay—CPT activity, apparent K_m for carnitine and palmitoyl-CoA and IC₅₀ value for malonyl-CoA, defined as the malonyl-CoA concentration that produces 50% inhibition of enzyme activity, were determined using mitochondria isolated from transformed yeasts, as previously reported (31).

Assessment of the Folding State of Human CPT1A Mutants—Folding state of the human CPT1A mutants was analyzed by proteolytic digestion (10 μ g/ml of trypsin) using intact or Triton X-100 (0.5% v/v) solubilized mitochondria (0.05 mg of protein/ml) as previously described for the rat protein (19, 31). Samples were analyzed by SDS-PAGE and immunoblotting.

Western Blot Analysis—Proteins were analyzed by SDS-PAGE (33) in an 8% gel and detected after blotting onto nitrocellulose as previously described (31) using the ECL detection system (Pierce) according to the supplier's instructions.

Chemicals—TaqDNA polymerase, as well as PCR and sequencing reagents were purchased from Applied Biosystems. Yeast culture media products were from Difco, and Zymolase 20T was from ICN Biomedicals, Orsay, France. Others chemicals were purchased from Sigma.

RESULTS

Molecular Analysis of Patient 2 and CPT1A Expression in Fibroblasts—As previously reported, three missense mutations were identified in patient 1: A275T and A414V carried on the paternal allele, and Y498C carried on the maternal allele (27). The present molecular analysis of patient 2 permitted to identify both the heterozygous 2126G>A substitution predictive of the G709E mutation, and the 948delG deletion, which corresponds to the R316fsX328 frameshift at codon 316 (exon 9) generating a stop signal 12 codons downstream (exon 10) (Fig. 1A). This latter mutation was identified in a heterozygous state at the gDNA level, whereas it was not detected at the cDNA level (Fig. 1A), pointing out the instability of the R316fsX328 mRNA (Fig. 1B). CPT1A immunodetection in fibroblasts from patients indicated that, by contrast to a previously described patient homozygous for the G710E mutation (patient 3) (26), neither patient 1 nor patient 2 expressed CPT1A protein at a detectable level (Fig. 2).

Wild-type and CPT1A Mutants Expression in *S. cerevisiae*—The functional analysis of mutations A275T, A414V, Y498C, and G709E was performed using heterologous expression in yeast *S. cerevisiae*, an eukaryotic organism devoid of endoge-

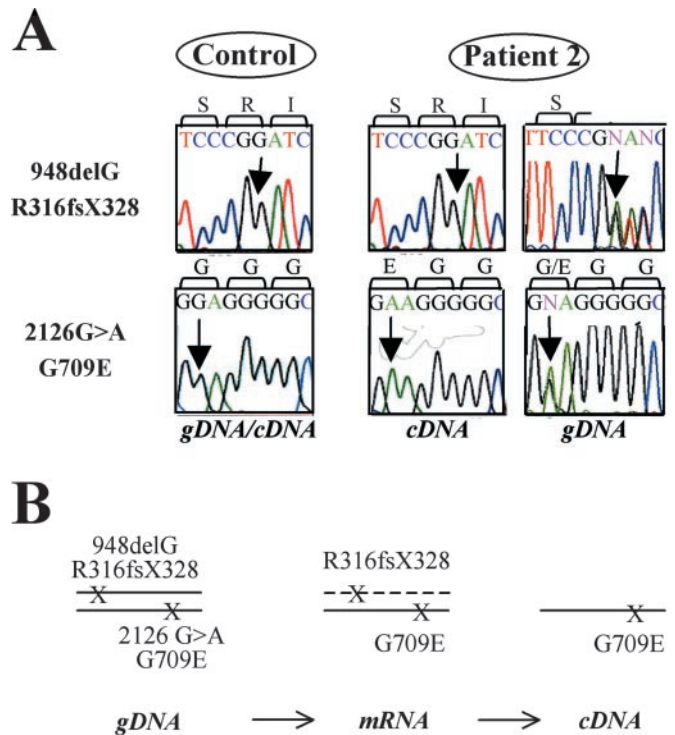


FIG. 1. Mutation analysis of the CPT1A gene in patient 2. A, partial sequences of CPT1A cDNA and gDNA of control and patient 2. B, schematic representation of the consequences at the mRNA and cDNA levels of these two CPT1A mutations.

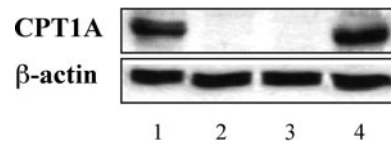


FIG. 2. Immunodetection of CPT1A in fibroblasts. Solubilized fibroblasts (100 μ g of protein) from control (lane 1), patient 1 carrying the heterozygous A275T, A414V, and Y498C mutations (lane 2), patient 2 carrying the heterozygous G709E and R316fsX328 mutations (lane 3), and a previously described patient carrying the homozygous G710E mutation (lane 4) were analyzed by SDS-PAGE electrophoresis and immunoblotting using rat CPT1A and human β -actin antibodies.

nous CPT1 activity (34), which was previously used for the functional analysis of the mutation G710E (26). Subcellular fractionation experiments did not reveal any change in the mitochondrial targeting of the yeast-expressed wild-type and CPT1A mutants (results not shown). CPT1A immunodetection using variable amounts of mitochondria isolated from the different yeast strains show that proteins of predicted sizes were synthesized with different levels of expression (Fig. 3). Wild-type and mutants A275T and G709E were expressed at a similar steady-state level. By contrast, mutant Y498C exhibited a 2-fold lower protein level in comparison to wild-type, indicating that this mutation led to a slight protein instability. For mutants A414V and A275T-A414V, the level of protein expression was 20–30-fold lower than wild-type, indicating that the A414V substitution alone or in combination with A275T conferred a dramatic protein instability. Despite the fact that some of these mutations affect CPT1A protein stability, enough expressed proteins was recovered in yeast mitochondria, in contrast to what was observed in fibroblasts (Fig. 2), to perform the functional analysis of these substitutions.

Enzyme Activity, Malonyl-CoA Inhibition, and Kinetic Properties of CPT1A Mutants—As shown in Table I, mutants A275T, Y498C, A414V, and A275T-A414V exhibited malonyl-CoA-sensitive CPT activity that was respectively 74, 46, 6, and

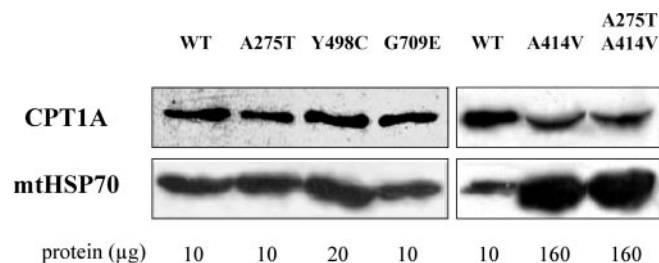


FIG. 3. **Heterologous expression of wild-type and CPT1A mutants in *S. cerevisiae*.** Mitochondria from the yeast strains expressing the wild-type (10 μg of protein), mutants A275T and G709E (10 μg of protein), Y498C (20 μg of protein), and A414V and A275T-A414V (160 μg of protein) were analyzed by SDS-PAGE electrophoresis and immunoblotting using rat CPT1A and yeast mitochondrial matrix mtHSP70 antibodies. WT, wild-type.

2% of that observed for the wild-type. For mutants Y498C, A414V, and A275T-A414V this decrease in CPT1 activity may partly result from the lower level of expressed protein (Fig. 3). As previously reported for mutant G710E (26), mutant G709E was totally inactive whatever the concentration of substrate employed (Table I, Fig. 4, B and D) despite similar level of CPT1A protein expression when compared with wild-type (Fig. 3). Mutations A275T and Y498C did not alter malonyl-CoA sensitivity, their IC_{50} value for malonyl-CoA being similar to that of the wild-type (Table I). Due to the low residual activity in mutants A414V and A275T-A414V, it was not possible to assess their malonyl-CoA sensitivity. All mutants, except mutant G709E, exhibited normal saturation kinetics when the carnitine concentration varied relative to a fixed concentration of palmitoyl-CoA (Fig. 4, A and B) or when palmitoyl-CoA concentration varied when the molar ratio of palmitoyl-CoA/albumin was fixed at 6.1:1 (Fig. 4, C and D). Mutation A275T was previously characterized in COS cells as a functionally neutral polymorphism (25). However, analysis of its saturation kinetics, which was not performed in the study of Brown *et al.* (25), indicated that this mutation decreased by 25% to 43% the V_{max} and catalytic efficiency (V_{max}/K_m) for carnitine and palmitoyl-CoA with no alteration in the apparent K_m for both substrates (Table I). In comparison to wild-type, mutant Y498C had a similar apparent K_m for palmitoyl-CoA but a 2-fold decrease in its apparent K_m for carnitine, indicating a slight increased affinity of the enzyme to this substrate. Moreover, mutant Y498C showed a 3-fold decrease in its V_{max} and catalytic efficiencies for carnitine and palmitoyl-CoA when compared with wild-type. Mutants A414V and A275T-A414V presented no alteration in the apparent K_m for carnitine and palmitoyl-CoA, but at least a 98% decrease in their V_{max} and catalytic efficiency whatever the substrate used (Table I). Thus, mutations A275T, Y498C, A414V, and A275T-A414V altered the V_{max} and the catalytic efficiency more than the K_m for carnitine and palmitoyl-CoA, whereas mutation G709E totally inactivated the enzyme.

Assessment of the Folding State of CPT1A Mutants—Previous works (14, 19, 31) showed that the rat CPT1A exhibits a native functional conformation characterized by a highly folded state resistant to trypsin proteolysis. When the outer mitochondrial membrane is disrupted, such as during the swelling procedure, trypsin is able to cleave the loop connecting TM1 and -2, hence generating an 82-kDa fragment. Moreover, the catalytic C-terminal domain of the rat CPT1A has been shown to contain a highly trypsin-resistant 60-kDa folded core that could be observed when solubilized mitochondria were submitted to trypsin proteolysis (14). As shown in Fig. 5A, the human wild-type CPT1A protein also remained largely resistant to trypsin treatment in intact mitochondria. The integrity of the outer

mitochondrial membrane was checked by the inaccessibility of cytochrome b2 to trypsin proteolysis (Fig. 5A). Mutants A275T and G710E, as well as mutants A414V and A275T-A414V (results not shown), exhibited the same protease resistance as the wild-type protein, whereas mutants Y498C and G709E were sensitive to trypsin proteolysis (Fig. 5A). When yeast mitochondria containing either the wild-type or the mutants A275T and G710E were solubilized by Triton X-100 in the presence of trypsin, both the 82- and 60-kDa fragments were detected (Fig. 5B, f1 and f2 fragments). These results strengthened the fact that the human CPT1A protein also contained within its catalytic C-terminal domain a highly folded trypsin-resistant core that was not affected by mutations A275T and G710E. By contrast, the generation of the f1 and f2 fragments was either less efficient or totally absent in the case of mutants Y498C and G709E (Fig. 5B), suggesting a partial unfolding of their C-terminal domain. The endogenous matrix soluble HSP70 protein (mtHSP70) was used as a positive control for trypsin proteolysis as its conformational states can be assessed by limited trypsin proteolysis (35).

Localization of Mutations in a Structure Model of Human CPT1A—To understand the possible molecular mechanism for the effects of these mutations on the catalytic activity and the conformation of the enzyme, we examined their locations in a structure model of human CPT1A. The model was created with the program MODELLER (36) based on the crystal structure of the mouse CAT (21), which shares 32% amino acid sequence identity with that of human CPT1A. Only residues 166–773 of human CPT1A have been used to build the structure model (Fig. 6A), as the first 160 residues of CPT1A do not have counterparts in CAT. This analysis indicates that residues Ala-275, Ala-414, Gly-709, and Gly-710 are in the core of the human CPT1A protein, whereas residue Tyr-498 is located in a surface loop which contains an inserted segment as compared with mouse CAT (Figs. 6A and 7).

Residues Ala-275, Ala-414, and Tyr-498 are located about 19, 24, and 43 Å from the active site, respectively (Fig. 6A). Ala-275 is in the middle of helix α_6 , and Ala-414 is near the end of helix α_{10} , in a tight turn linking this helix to strand β_6 (Fig. 6A). Their location at more than 20 Å away from the active site suggests an indirect mechanism for the deleterious effects of the corresponding mutations. In addition, these mutations have small effects on the K_m of the enzyme (Table I), indicating that substrate binding is not significantly affected in these mutants. On the other hand, their altered V_{max} (Table I) suggest that the main effect of these mutations was to decrease the stability of the enzyme-substrate complex and/or of the CPT1A protein itself (Fig. 3).

Concerning residues Gly-709 and Gly-710, the structure analysis of human CPT1A shows that these residues are located near the active site of the enzyme within the conserved strand β_{14} (Fig. 6A). Moreover, they have opposite location relative to the plane of strand β_{14} , and the long-chain acyl-CoA and carnitine binding sites (Fig. 6B). Modeling studies of the mutations G709E and G710E are illustrated in Fig. 6B. Replacement of Gly-709 by a Glu residue leads to the introduction of a bulky and negatively charged group in the hydrophobic core of the enzyme. For the G710E mutation, this negatively charged Glu residue is in the vicinity of the catalytic His-473 residue (7 Å) and of the carnitine molecule (10 Å) (Fig. 6B), and causes a drastic alteration in the hydrophobic pocket of the enzyme. In conclusion, the loss of activity observed for mutants G709E and G710E can be explained by their strategic location in the catalytic machinery.

TABLE I

Enzyme activity, malonyl-CoA inhibition and kinetic parameters of the wild-type and mutants CPT1A expressed in *S. cerevisiae*

Mitochondria were isolated from the yeast strains separately expressing wild-type and mutants CPT1A. CPT activity was assayed with 80 μM palmitoyl-CoA and 200 μM carnitine in the absence or presence of 150 μM malonyl-CoA. Numbers in parentheses represent the percentage of catalytic efficiency (V_{max}/K_m) compared to that of the wild-type (100%). ND, not determined.

Strain	Activity		Malonyl-CoA		Carnitine		Palmitoyl-CoA		Catalytic efficiency	
	-Malonyl-CoA	+Malonyl-CoA	IC ₅₀	K _m	V _{max}	K _m	V _{max}	Carnitine	Palmitoyl-CoA	
	nmol/min/mg		μM	μM	nmol/min/mg	μM	nmol/min/mg	V_{max}/K_m	V_{max}/K_m	
Wild-type	6.5 ± 0.6	0.8 ± 0.08	1.83 ± 0.4	106.5 ± 8.4	147.8 ± 10.5	82.8 ± 9.4	88.6 ± 10.2	1.4 (100%)	1.07 (100%)	
A275T	4.8 ± 0.3	0.4 ± 0.08	1.70 ± 0.32	107.4 ± 16.8	87.0 ± 10.5	75.5 ± 8.3	61.1 ± 13.2	0.8 (60%)	0.8 (76%)	
A414V	0.4 ± 0.05	0.05 ± 0.03	ND	78.0 ± 8.0	1.6 ± 0.1	54.2 ± 4.2	1.1 ± 0.1	0.02 (1.5%)	0.02 (1.9%)	
A275T-A414V	0.13 ± 0.04	0.04 ± 0.02	ND	96.7 ± 2.9	0.6 ± 0.1	55.5 ± 3.5	0.4 ± 0.1	0.006 (0.5%)	0.007 (0.7%)	
Y498C	3.0 ± 0.2	0.2 ± 0.01	1.53 ± 0.06	61.3 ± 6.8	29.2 ± 1.3	66.3 ± 9.5	25.9 ± 5.6	0.5 (34%)	0.4 (37%)	
G709E	Undetectable	Undetectable	ND	ND	ND	ND	ND	ND	ND	

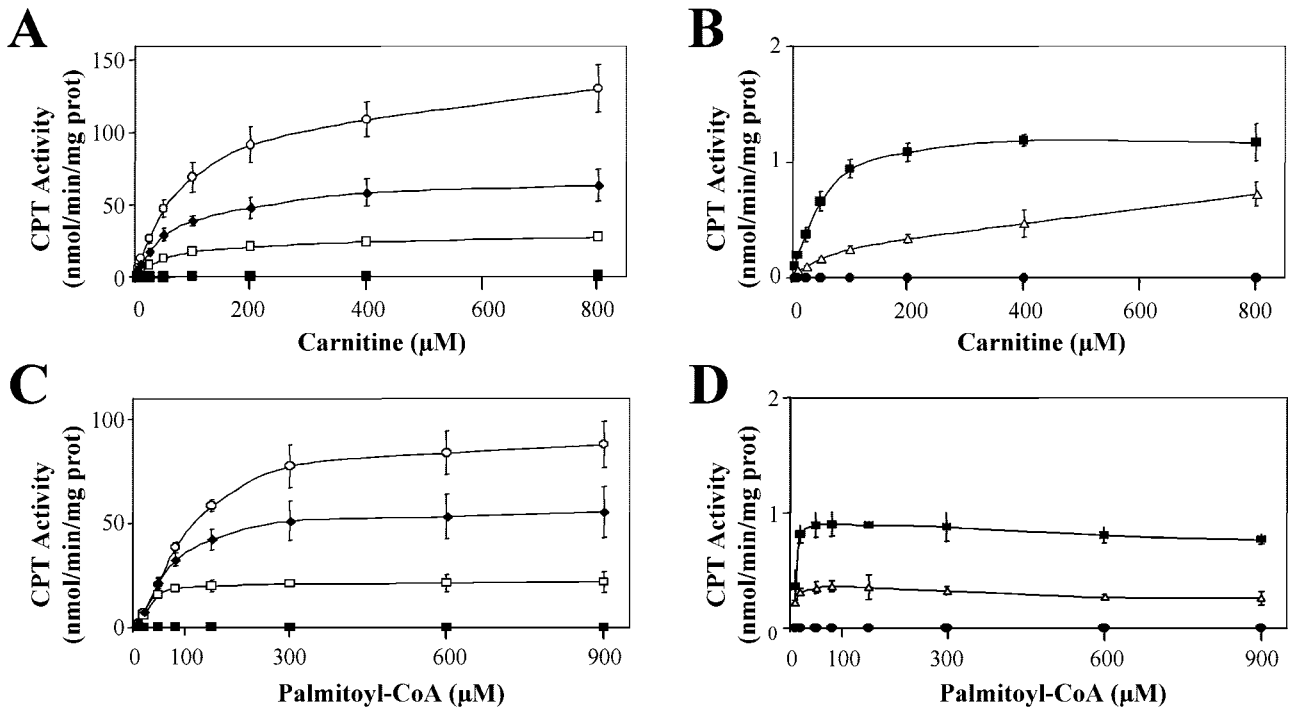


FIG. 4. Kinetic analysis of wild-type and CPT1A mutants. Isolated mitochondria from the yeast strains expressing the wild-type CPT1A (○), A275T (◆), Y498C (□), A414V (■), A275T-A414V (△), and G709E (●) mutants were assayed for CPT activity in the presence of increasing concentrations of carnitine (A and B) and palmitoyl-CoA (C and D). Results are the mean ± S.E. of three to six separate experiments.

DISCUSSION

In the present study, combined functional and structural approaches allowed to validate the A275T, A414V, Y498C, and G709E substitutions as disease-causing mutations in human CPT1A and to investigate for the first time the molecular mechanisms responsible for their deleterious effects.

Substitution of the non-polar Ala-275 residue by an uncharged-polar residue could lead to more serious consequences. However, Ala-275 is not conserved among the acylcarnitine transferase family and several members, such as rat and mouse CPT1A, have a natural threonine at this codon (Fig. 7). Investigation of the protein conformational state by trypsin proteolysis experiments established that the human CPT1A protein contains within its catalytic C-terminal domain a highly folded trypsin-resistant core, as reported previously for the rat protein (12, 14). This intrinsic property of CPT1A constitutes a valuable criterion to detect important conformational change that would unmask buried trypsin cleavage sites. Despite that mutant A275T did not exhibit such a conformational change, its protein structure might be slightly disrupted by the replacement of a small residue into a longer one because this mutation occurs within helix α_6 that is a central element essential for the protein structure. Therefore, we hypothesized that this small structure perturba-

tion could alter the organization of the catalytic core, hence leading to the observed decreased activity. Recently, His-277 in rat CPT1A was suggested to be involved in the malonyl-CoA high affinity site (17). Despite the proximity of Ala-275 and His-277 within helix α_6 , mutant A275T exhibits normal malonyl-CoA sensitivity, indicating that this residue is not critical for malonyl-CoA inhibition.

The dramatic effects of mutation A414V, *i.e.* a severe protein instability and a 98% decrease in catalytic efficiencies, were surprising given that this substitution did not modify the non-polar nature of the lateral chain. However, Ala-414 is conserved in all CPT isoforms (Fig. 7), and the presence of a serine in both carnitine octanoyltransferase and CAT as well as a cysteine in choline acetyltransferase (Fig. 7) indicates the requirement of a small residue at this position. Moreover, our three-dimensional structure model shows that this residue, located 24 Å from the active site, constitutes a tight link between helix α_{10} and strand β_6 . Modeling studies suggest that introduction of a larger Val side chain at this position will cause steric clashes among the neighboring residues, requiring conformational changes in this region. It may be possible that changes in the positioning of strand β_6 are transmitted via the intermediate β -sheets to strand β_8 , which is closely linked to

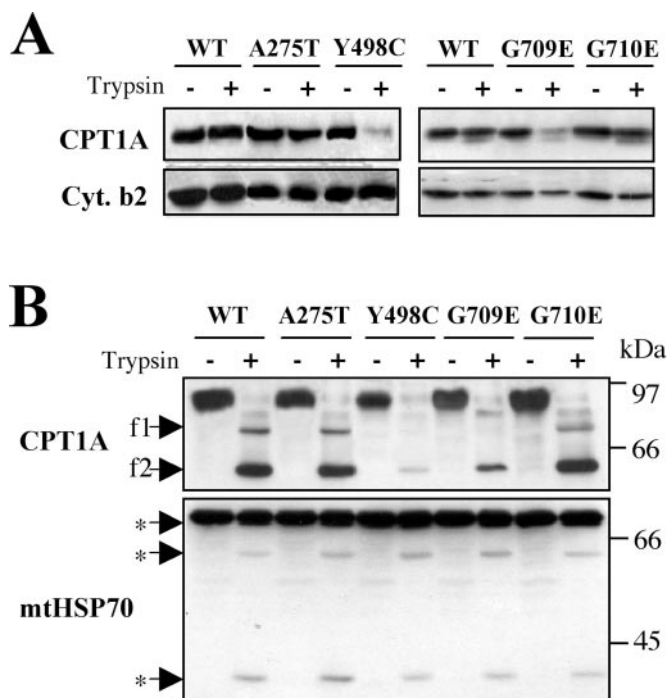


FIG. 5. Trypsin-resistant conformational state of yeast-expressed wild-type and CPT1A mutants in intact (A) or Triton X-100 solubilized (B) mitochondria. Samples were analyzed by SDS-PAGE electrophoresis and immunoblotting using anti-rat CPT1A and yeast cytochrome b2 (*Cyt. b2*) or yeast mtHSP70 antibodies. *f1* and *f2* denote the respective 82- and 60-kDa fragments of human CPT1A generated by trypsin, and the *asterisks* represent the trypsin proteolytic fragments of yeast mtHSP70. Results are representative of at least three different experiments with separate mitochondrial preparations. WT, wild-type.

the catalytic His residue (Fig. 6A). This would result in the destabilization of the whole catalytic core, altering both protein stability and enzymatic activity. Functional analysis of the double mutant A275T-A414V (as these two mutations were carried by the same allele in patient 1) showed that the V_{max} and catalytic efficiencies were slightly more affected in comparison to mutant A414V, suggesting that mutation A275T emphasized the pathogenic character of mutation A414V.

Y498C was shown to be responsible for a slight protein instability, a 3-fold decrease in the V_{max} and catalytic efficiencies for both carnitine and palmitoyl-CoA, and a 2-fold increase in the affinity for carnitine. As Tyr-498 is located at more than 40 Å from the active site (Fig. 6A), its deleterious effects are indirect and may result from an altered conformation, as indicated by the trypsin proteolysis experiments (Fig. 5). Nevertheless, it is difficult to predict the exact behavior of this mutated residue because it is located in the loop connecting helix $\alpha 12$ and strand $\beta 9$ that contains an inserted segment in CPT1A compared with CAT (Figs. 6A and 7). Despite being on the external face of the protein, this loop is likely to play a structural role, strengthening the importance of protein conformation for the functionality of the enzyme.

Functional analysis of the G709E mutation, which behaves as in a hemizygous state in patient 2, was particularly interesting because this mutation resulted in protein instability in patient fibroblasts whereas the previously reported G710E mutation did not (Fig. 2). Both G709E and G710E mutants were totally inactive (present study and Ref. 26), but only G709E mutant exhibited a trypsin-sensitive conformation. Thus, protein unfolding of G709E mutant explained the protein instability observed in fibroblasts. Residues Gly-709-Gly-710 are conserved among all the CPT1 isoforms and are adjacent to a

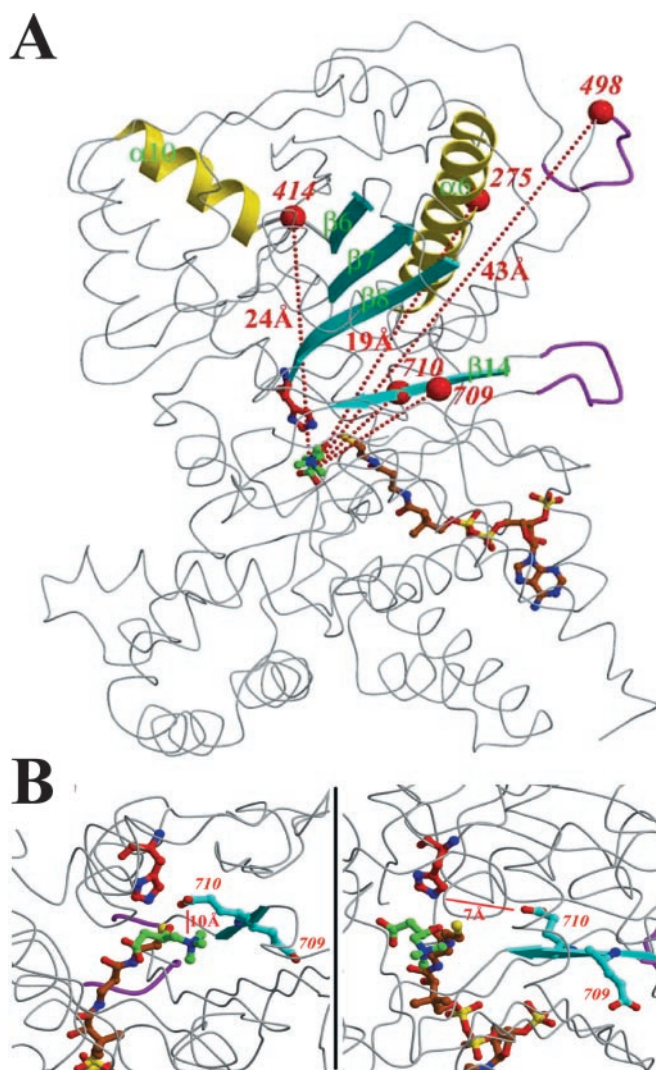


FIG. 6. Localization of the mutations in a structure model of human CPT1A. A, the structure model of residues 166–773 of human CPT1A (excluding the N-terminal domain) is shown as a *thin trace* in gray. The two inserted segments relative to mouse CAT are shown in magenta. The catalytic His473 residue, carnitine, and CoA are shown as *stick models* in red, green, and orange for carbon atoms, respectively. The mutation sites are indicated with red spheres, and their distances to the carnitine molecule are indicated. B, the active site region of the human CPT1A model in two views, showing the positions of the G709E and G710E mutations. The distances of G710E to the catalytic His-473 and carnitine are indicated.

Gly-Phe-Gly pattern (Fig. 7), previously suggested to be involved in carnitine binding in rat CPT2 (37). They are equivalent to Val-563-Met-564 in CAT (Fig. 7) and are located near the end of strand $\beta 14$, in the immediate vicinity of the carnitine molecule (Fig. 6, A and B). The side chain of the Val-563 residues within the hydrophobic pocket of the catalytic core of the CAT, pointing away from carnitine. Modeling studies showed that its replacement by the small Gly residue in the CPT1A, together with several other amino acid changes in this region, would produce a cavity in the core. It is therefore likely that the position of strand $\beta 14$ will move slightly, away from carnitine, to fill this void, keeping Gly-709 in the hydrophobic core of the structure. Based on this model, the large effects of the G709E mutation on the stability of CPT1A can be explained by the introduction of a bulky and negatively charged group in the hydrophobic core of the enzyme, causing steric repulsions as well as unfavorable electrostatic interactions (Fig. 6B).

Concerning the Gly-710 residue, structural analysis showed

	275 *	414	498	709-710
CPT1A human	ARA-GNA I HAIL	DAVEKA A FFVT	SLQLG V AEDGH	EYVSS GG FGFPV
rat	ARA-GNT I HAIL	DAVEKA A FFVT	VFQLG V SEDGH	DYVSC GG FGFPV
mouse	ARA-GNT I HAIL	DAVEKA A FFVT	VFQLG V SEDGH	DYVSC GG FGFPV
CPT1B human	ARL-GN I IHAM I	EAIERA A FFV A	SFHLG V TETGH	NHLGA GG FGFPV
rat	ARL-GNT V HAM I	DTIERA A FFV A	TFHLG V TETGH	NHLGA GG FGFPV
mouse	ARL-GN A VHAM I	DAIERA A FFV T	TFHLG V TETGH	NHLGA GG FGFPV
CPT1C human	ARA-GN A VHALL	EAVEGA A FFV S	CFQLG V STDGH	DYVSS GG FGFPV
mouse	ARA-GN A VHTLL	EAVEGA A FFV S	CFQLG V ATDGH	DYVSS GG FGFPV
CPT2 human	TRATNM I VSA-I	RKVDS A VFC L C	TQTPAV T PQ S Q	SPAVN L GGFAPV
rat	TRATNL T VSA-V	KKVDS A VFC L C	TQTPAI T PQ S Q	SPAVS L GGFAPV
mouse	TRATNL T VSA-V	RKVDS A VFC L C	TQTPAI A PQ S Q	SPAVS L GGFAPV
COT human	ERGSITL W HN-N	EKIQ S LLV V S	FQNEGR W KG--	-YLRV Q GVV V PM
rat	ERGSILL W HN-N	EKIQ S S L EV V S	LETEGR W KG--	-YLRI Q GVV V PM
CAT human	RFAAK L IEGV-L	RSIQ S I F TV C	K-----K P E	AKTDC V M F FG P V
mouse	RFAAK L IEGV-L	NSIQ S I F TV C	K-----K P E	AKTDC V M F FG P V
ChAT human	RFAAS L ISGV-L	DMIER C IC L V C	TQ----SS R KL	TTTEM F CC Y GPV
rat	RFAAC L ISGV-L	DMIER C IC L V C	MT----SN K KL	TTMEM F CC Y GPV

FIG. 7. Sequence alignment of regions surrounding the human mutated CPT1A residues of various acyltransferases. Corresponding amino acids are boxed when conserved. Identical conserved residues are shaded. *, conserved His-277 in all malonyl-CoA sensitive enzymes; COT, carnitine octanoyltransferase; CAT, carnitine acetyltransferase; ChAT, choline acetyltransferase.

that this residue is in the active site, facing both the catalytic His residue and the carnitine molecule (Fig. 6B). However, our modeling studies of the G710E mutation indicated that the negatively charged Glu residue is physically unable to interfere with the catalytic His residue and/or to balance the positive charge of the trimethylammonium group of carnitine (Fig. 6B). We have suggested earlier that its equivalent in CAT, Met-564, partly fills the hydrophobic pocket, and hence allows the access to the binding site for only acetyl-CoA and not for the palmitoyl group (21). In addition to the movement of the strand β 14 discussed above, the presence of a Gly residue at this position in CPT1A also contributes to create additional space for binding the long acyl chains. This is reinforced by the fact that the Gly-710 residue is conserved in all the long- and medium-chain acyltransferases (Fig. 7). Therefore, the functional inactivity of mutant G710E can be explained by the fact that the bulkier Glu side chain blocks the binding of long-chain acyl groups. Altogether, these results demonstrate that both Gly-709-Gly-710 residues are essential for enzymatic activity because they are structurally part of the hydrophobic core of the catalytic site. Moreover, this illustrates that residues located far from the catalytic residues in the primary amino acid sequence can in fact be crucial elements of the catalytic core. This also explains why deletion and/or mutation within the C terminus of CPT1A so dramatically affected initial protein folding and/or catalytic activity (19, 20).

In conclusion, these combined functional and structural analyses of missense mutations in CPT1A deficiency provide novel insights into the functionality of this enzyme. Firstly, this work demonstrates that disease-causing mutations in CPT1A can be roughly divided into two categories depending on whether they affect directly (functional determinant) or indirectly the active site of the enzyme (structural determinant). Mutations A275T, A414V, and Y498C clearly belong to the second class, as they are located at more than 20 Å away from the active site and affected more the stability of the protein itself and/or of the enzyme-substrate complex than the K_m for the substrates. By contrast, mutations G709E and G710E belong to the first category. Indeed, these small Gly residues are not only essential for the structure of the hydrophobic core in the catalytic site, but also contribute to the structural basis for the selectivity of long-chain acyl-CoA. This

illustrates that significant structural differences between CAT and CPT1A are indeed underlying structural bases for their kinetic specificity. Finally, it is also clear from structural modeling studies that human CPT1A has outside its active site significant insertions in several of the surface loops, such as the one containing Tyr-498, as compared with CAT. These secondary structural elements may form additional interactions within the catalytic domain. However, the functional exploration of these secondary structural elements of CPT1A, as well as of the interactions between its N- and C-terminal domains reported to modulate the degree of malonyl-CoA sensitivity (38), requires the specific crystal structure of the CPT1A enzyme.

Acknowledgments—We are grateful to the referring physicians and F. Demaugre (INSERM U370, Paris, France) for patient tracking. We thank W. Neupert (Munich, Germany) for the antibodies against the yeast cytochrome b2 and HSP70 and N. Kadhon (INSERM U393) for cell culture.

REFERENCES

- McGarry, J. D., and Brown, N. F. (1997) *Eur. J. Biochem.* **244**, 1–14
- Ramsay, R. R., Gandour, R. D., and van der Leij, F. R. (2001) *Biochim. Biophys. Acta* **1546**, 21–43
- Prentki, M., and Corkey, B. E. (1996) *Diabetes* **45**, 273–283
- Zammit, V. A. (1999) *Biochem. J.* **343**, 505–515
- Ruderman, N. B., Saha, A. K., Vavvas, D., and Witters, L. A. (1999) *Am. J. Physiol.* **276**, E1–E18
- Unger, R. H., and Orci, L. (2001) *Faseb J.* **15**, 312–321
- McGarry, J. D. (2002) *Diabetes* **51**, 7–18
- Britton, C. H., Schultz, R. A., Zhang, B., Esser, V., Foster, D. W., and McGarry, J. D. (1995) *Proc. Natl. Acad. Sci. U. S. A.* **92**, 1984–1988
- Yamazaki, N., Shinohara, Y., Shima, A., Yamanaka, Y., and Terada, H. (1996) *Biochim. Biophys. Acta* **1307**, 157–161
- Price, N., van der Leij, F., Jackson, V., Corstorphine, C., Thomson, R., Sorensen, A., and Zammit, V. (2002) *Genomics* **80**, 433–442
- Fraser, F., Corstorphine, C. G., and Zammit, V. A. (1997) *Biochem. J.* **323**, 711–718
- Cohen, I., Kohl, C., McGarry, J. D., Girard, J., and Prip-Buus, C. (1998) *J. Biol. Chem.* **273**, 29896–29904
- Shi, J., Zhu, H., Arvidson, D. N., and Woldegiorgis, G. (1999) *J. Biol. Chem.* **274**, 9421–9426
- Cohen, I., Guillerault, F., Girard, J., and Prip-Buus, C. (2001) *J. Biol. Chem.* **276**, 5403–5411
- Ijlst, L., Mandel, H., Oostheim, W., Ruiters, J. P., Gutman, A., and Wanders, R. J. (1998) *J. Clin. Invest.* **102**, 527–531
- Morillas, M., Gomez-Puertas, P., Roca, R., Serra, D., Asins, G., Valencia, A., and Hegardt, F. G. (2001) *J. Biol. Chem.* **276**, 45001–45008
- Morillas, M., Gomez-Puertas, P., Rubi, B., Clotet, J., Arino, J., Valencia, A., Hegardt, F. G., Serra, D., and Asins, G. (2002) *J. Biol. Chem.* **277**, 11473–11480
- Morillas, M., Gomez-Puertas, P., Bentebibel, A., Selles, E., Casals, N., Valen-

- cia, A., Hegardt, F. G., Asins, G., and Serra, D. (2003) *J. Biol. Chem.* **278**, 9058–9063
19. Pan, Y., Cohen, I., Guillerault, F., Feve, B., Girard, J., and Prip-Buus, C. (2002) *J. Biol. Chem.* **277**, 47184–47189
20. Treber, M., Dai, J., and Woldegiorgis, G. (2003) *J. Biol. Chem.* **278**, 11145–11149
21. Jogl, G., and Tong, L. (2003) *Cell* **112**, 113–122
22. Wu, D., Govindasamy, L., Lian, W., Gu, Y., Kukar, T., Agbandje-McKenna, M., and McKenna, R. (2003) *J. Biol. Chem.* **278**, 13159–13165
23. Bougneres, P. F., Saudubray, J. M., Marsac, C., Bernard, O., Odievre, M., and Girard J. R. (1980) *N. Engl. J. Med.* **302**, 123–124
24. Bonnefont, J. P., Demaugre, F., Prip-Buus, C., Saudubray, J. M., Brivet, M., Abadi, N., and Thuillier, L. (1999) *Mol. Genet. Metab.* **68**, 424–440
25. Brown, N. F., Mullur, R. S., Subramanian, I., Esser, V., Bennett, M. J., Saudubray, J. M., Feigenbaum, A. S., Kobari, J. A., Macleod, P. M., McGarry, J. D., and Cohen, J. C. (2001) *J. Lipid Res.* **42**, 1134–1142
26. Prip-Buus, C., Thuillier, L., Abadi, N., Prasad, C., Dilling, L., Klasing, J., Demaugre, F., Greenberg, C. R., Haworth, J. C., Droin, V., Kadhon, N., Gobin, S., Kamoun, P., Girard, J., and Bonnefont, J. P. (2001) *Mol. Genet. Metab.* **73**, 46–54
27. Gobin, S., Bonnefont, J. P., Prip-Buus, C., Mugnier, C., Ferrec, M., Demaugre, F., Saudubray, J. M., Rostane, H., Djouadi, F., Wilcox, W., Cederbaum, S., Haas, R., Nyhan, W. L., Green, A., Gray, G., Girard, J., and Thuillier, L. (2002) *Hum. Genet.* **111**, 179–189
28. Ogawa, E., Kanazawa, M., Yamamoto, S., Ohtsuka, S., Ogawa, A., Ohtake, A., Takayanagi, M., and Kohno, Y. (2002) *J. Hum. Genet.* **47**, 342–347
29. Schaefer, J., Jackson, S., Taroni, F., Swift, P., and Turnbull, D. M. (1997) *J. Neurol. Neurosurg. Psychiatry* **62**, 169–176
30. Saudubray, J. M., Coude, F. X., Demaugre, F., Johnson, C., Gibson, K. M., and Nyhan, W. L. (1982) *Pediatr. Res.* **16**, 877–881
31. Prip-Buus, C., Cohen, I., Kohl, C., Esser, V., McGarry, J. D., and Girard, J. (1998) *FEBS Lett.* **429**, 173–178
32. Lowry, O. H., Rosebrough, N. J., Lewis Farr, A., and Randall, R. J. (1951) *J. Biol. Chem.* **193**, 265–275
33. Laemmli, U. K. (1970) *Nature* **227**, 680–685
34. Brown, N. F., Esser, V., Foster, D. W., and McGarry, J. D. (1994) *J. Biol. Chem.* **269**, 26438–26442
35. Fung, K. L., Hilgenberg, L., Wang, N. M., and Chirico, W. J. (1996) *J. Biol. Chem.* **271**, 21559–21565
36. Sali, A., and Blundell, T. L. (1993) *J. Mol. Biol.* **234**, 779–815
37. Brown, N. F., Anderson, R. C., Caplan, S. L., Foster, D. W., and McGarry, J. D. (1994) *J. Biol. Chem.* **269**, 19157–19162
38. Jackson, V. N., Cameron, J. M., Fraser, F., Zammit, V. A., and Price, N. T. (2000) *J. Biol. Chem.* **275**, 19560–19566